

# Dual-Band Filter Power Divider with Controllable Transmission Zero Based on Multimode Resonator

Chuanyun Wang, Xiqiang Zhang\*, Tingting Xia, Yonghua Zhang, and Qilei Fan

**Abstract**—A novel dual-band filter power divider (DB-FPD) with controllable transmission zeros (TZs) is designed using a slotline multimode resonator (SLMR) in this letter. Using the stub loading technology, each resonator mode of the SLMR can be easily controlled. Accordingly, a dual-band bandpass filter is realized. Four TZs are generated due to the loaded stubs on the SLMR and feeding network, which can improve the out-of-band selectivity. Finally, without introducing additional circuits, a DB-FPD with good performance is realized. For verification, a prototype operating at 2.01 and 4.79 GHz is fabricated and measured. The measured results are basically consistent with simulated ones. The 3-dB fractional bandwidths are 29.7% (1.72 ~ 2.32 GHz) and 7.99% (4.58 ~ 4.96 GHz), respectively, and the isolation in each band is better than 14 dB.

## 1. INTRODUCTION

In wireless communication systems, the multi-functional integration to achieve the compactness of devices has become one of the current research hotspots of radio frequency (RF) devices [1, 2]. Filters and power dividers (PD) are indispensable components of RF circuits, and their integrated design, that is filter power divider (FPD), has also received attention. At present, there are mainly two methods for the design of FPD: the direct cascade between the filter and the PD [3, 4], and the integrated design of the filter and the PD. The former has the advantages of simple circuit structure, but the size of the circuit is inevitably increased, and the latter not only realizes the miniaturization of the circuit, but also reduces the additional insertion loss, which has become a popular method for the design of FPDs. For example, to meet the requirements of the miniaturization and low insertion loss, a novel three-way FPD based on SIW is designed in [5] by integrating slotline-microstrip structures with resonant cavities. However, multiple application scenarios not only require miniaturization of the FPD circuit, but also need dual-/multi-band functions. Single or multiple resonators can be used to design dual-/multi-band FPDs. In [6] and [7], multiple resonator structures are used to realize dual-band FPDs. On the other hand, multiple resonators will inevitably increase the difficulty of circuit design and impedance matching to a certain degree. In [8] and [9], a multimode resonator is used to implement FPDs design, respectively. In this way, the functions of power distribution and filtering response of the dual-band FPDs are simultaneously achieved, and the insertion loss is effectively reduced. Although these works show good performance, the out-of-band selection performance and bandwidth need to be improved. Therefore, for dual-/multi-band FPDs, in addition to meeting miniaturization requirements, bandwidth and out-of-band suppression level of each passband should be considered.

In this letter, a novel DB-FPD based on the integrated design method is designed. A slotline multimode resonator (SLMR) is introduced to obtain the functions of dual-band filter and power distribution simultaneously. A modified WPD and the SLMR are vertically cascaded, which can effectively decrease the circuit size. By adjusting the coupling strength between the resonant modes of

---

*Received 9 April 2022, Accepted 30 May 2022, Scheduled 23 June 2022*

\* Corresponding author: Xiqiang Zhang (xqzhang1005@163.com).

The authors are with the School of Information Engineering, East China Jiaotong University, Nanchang 330013, China.

the SLMR, a wider dual-band response is achieved. For improving the out-of-band selectivity of the DB-FPD, four controllable transmission zeros (TZs) are introduced on both sides of each passband. In addition, through introducing two isolation resistances, good isolation is achieved in each passband of the proposed DB-FPD.

## 2. DESIGN AND ANALYSIS OF MULTIMODE BANDPASS FILTER

The architecture of the proposed slotline bandpass filter is shown in Fig. 1(a). It mainly consists of a slotline stepped impedance resonator loaded with stubs, which can achieve the effect of multimode resonance. The physical length and width of the slotline are expressed by  $L_{Si}$  and  $W_{Si}$ , respectively, and the corresponding electrical length and characteristic admittance are represented by  $\theta_i$  and  $Y_i$  respectively ( $i = 1, 2 \dots$ ). Among them,  $\theta_1 = \beta L_{s1}$ ,  $\theta_2 = \beta L_{s2}$ ,  $\theta_3 = \beta L_{s3}$ ,  $\theta_4 = \beta L_{s4}$ , where  $\beta$  is the phase shift constant. The frequency response of the filter is shown in Fig. 1(b). It can be seen that the filter has four resonant modes, and two TZs are generated due to the loaded stub on the SLMR. By adjusting the coupling strength between the modes, dual-band effect can be achieved.

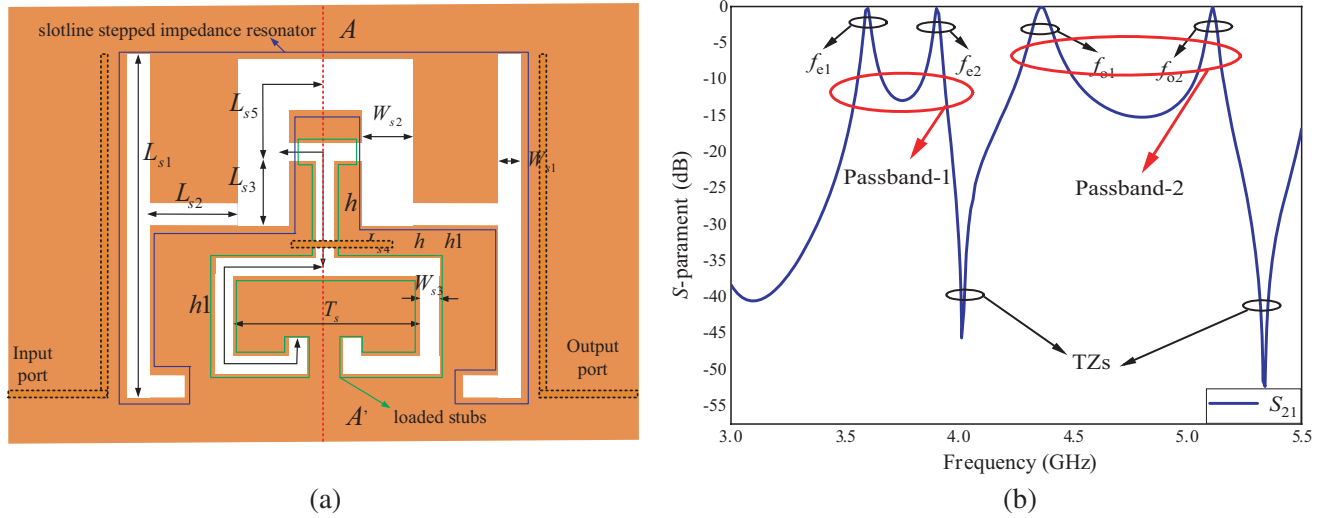


**Figure 1.** Configuration and simulation results of dual-band bandpass filter. (a) Configuration of the proposed filter. (b) Simulation results of  $S_{21}$ .

Since the SLMR is symmetrical about the center line  $AA'$ , odd- and even-mode analysis method can be utilized to analyze its resonance property [10, 11]. According to current distribution of the proposed SLMR under odd- and even mode excitation, it can be found that the odd- and even-mode equivalent circuits of the proposed SLMR and its corresponding microstrip form are dual [12]. The detailed analysis is as below.

As shown in Fig. 2(a), in the case of odd-mode excitation, the symmetry plane  $AA'$  can be regarded as an ideal electric wall, and the input admittance can be described by:

$$Y_{in,odd} = Y_1 \frac{Y_{ino1} + jY_1 \tan \theta_1}{Y_1 + jY_{ino1} \tan \theta_1} \quad (1)$$

of which:

$$Y_{ino1} = Y_1 \frac{Y_{ino2} + jY_1 \tan \theta_2}{Y_1 + jY_{ino2} \tan \theta_2} \quad (2)$$

$$Y_{ino2} = Y_2 \frac{Y_{ino3} + jY_2 \tan \theta_3}{Y_2 + jY_{ino3} \tan \theta_3} \quad (3)$$

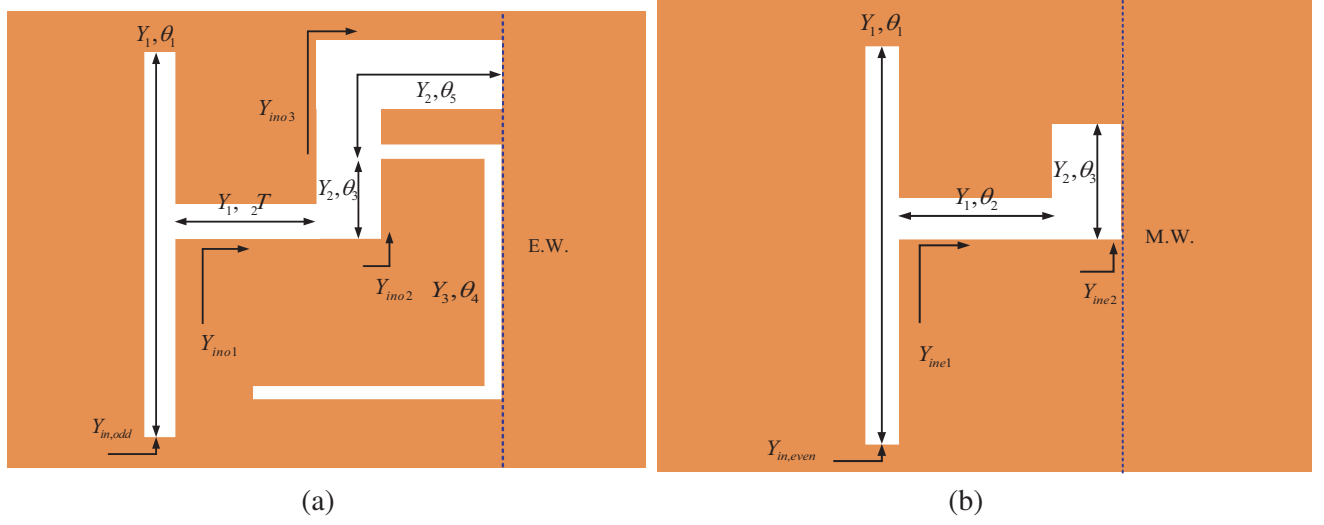


**Figure 2.** Odd- and even-mode equivalent circuit of multimode resonator. (a) Odd-mode equivalent circuit. (b) Even-mode equivalent circuit.

For the convenience of analysis, assume that  $Y_2 = Y_3$ ,  $\theta_4 = \theta_5 = \theta$ , then:

$$Y_{ino3} = jY_2 \frac{2 \tan \theta - \tan^2 \theta}{1 - 2 \tan \theta} \quad (4)$$

where  $\theta_i = 2\pi f L_i \sqrt{\varepsilon_r} / c$ ,  $c$  is the speed of light in free space, and  $\varepsilon_r$  is the effective dielectric constant. As shown in Fig. 2(b), the symmetry plane  $AA'$  can be regarded as an ideal magnetic wall under even-mode excitation. The input admittance can be described by:

$$Y_{in,even} = \frac{Y_{ine1} + jY_1 \tan \theta_1}{Y_1 + jY_{ine1} \tan \theta_1} \quad (5)$$

of which:

$$Y_{ine1} = \frac{Y_{ine2} + jY_1 \tan \theta_2}{Y_1 + jY_{ine2} \tan \theta_2} \quad (6)$$

$$Y_{ine2} = -jY_3 \cot \theta_3 \quad (7)$$

From the above analysis, it can be found that according to formulas (1)–(4), the two modes of  $f_{o1}$  and  $f_{o2}$  can be adjusted respectively by changing parameters  $\theta_1$ ,  $\theta_2$ ,  $\theta_3$ ,  $\theta_4$ , and  $\theta_5$  of the SLMR, which can form passband-2. According to formulas (5)–(7), by changing parameters  $\theta_1$ ,  $\theta_2$ , and  $\theta_3$  of the SLMR, the two modes of  $f_{e1}$  and  $f_{e2}$  are adjusted respectively, which is used to form passband-1. Therefore, in the final design, when the values of  $f_{e1}$  and  $f_{e2}$  in passband-1, i.e.,  $\theta_1$ ,  $\theta_2$  and  $\theta_3$ , are determined, the required  $f_{o1}$  and  $f_{o2}$  can be obtained by adjusting parameters  $\theta_4$  and  $\theta_5$ , so passband-2 is formed, and then dual-band filter is realized. The correctness of the design is verified by using software Sonnet, and due to space limitations, the simulation results are not attached here.

### 3. ANALYSIS AND DESIGN OF THE DB-FPD

As shown in Fig. 3(a), the configuration of the proposed DB-FPD is presented. It consists of an SLMR and a modified microstrip WPD. In order to make the DB-FPD have better isolation performance in both passbands, two isolation resistors  $R_1$  and  $R_2$  are introduced. To explain the principle of DB-FPD, the coupling topology is introduced as shown in Fig. 3(b).  $E_1$  and  $E_2$  represent two even-modes of the SLMR, respectively, which can form passband-1, and  $O_1$  and  $O_2$  represent two odd-modes, respectively, which are used to form passband-2. It can be clearly seen that the input signal is transmitted along the common input line at port 1, and then equally allocated to port 2 and port 3 through the coupling function of the SLMR.

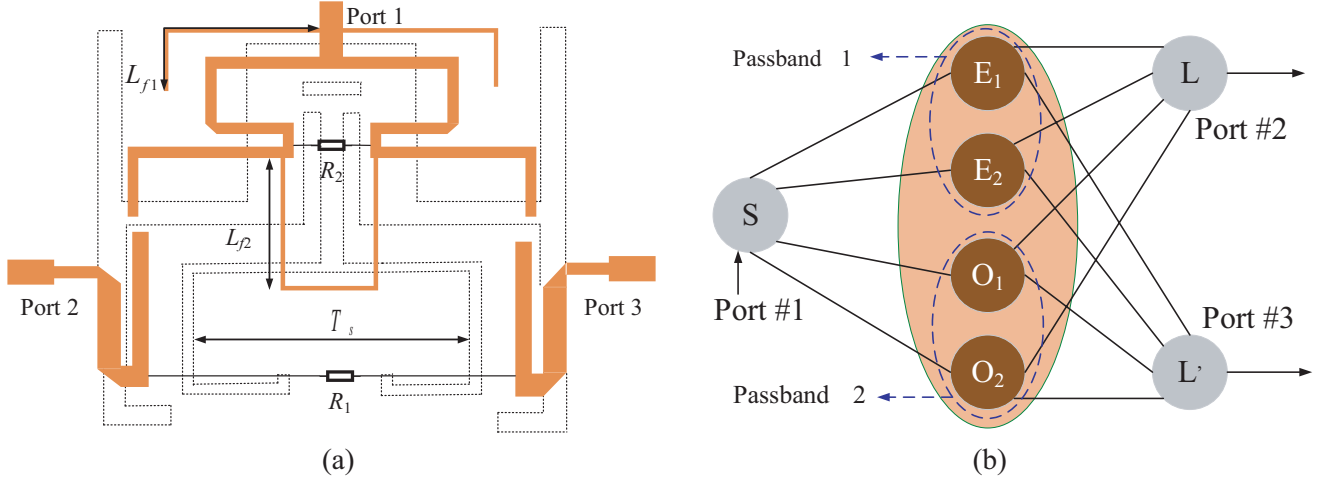


**Figure 3.** Configuration and coupling topology of DB-FPD. (a) Configuration of DB-FPD. (b) Coupling topology.

According to formulas (1)–(7) and parameter optimization with the help of the simulation software Sonnet, the main design parameters of the DB-FPD are determined and are listed in Table 1.

**Table 1.** Main design parameters of DB-FPD (mm).

$L_{S1}$	$L_{S2}$	$L_{S3}$	$L_{S4}$	$L_{S5}$	$W_{s1}$	$W_{s2}$	$W_{s3}$	$L_{f1}$	$L_{f2}$
25.3	7.4	10.7	30.85	2.5	1.5	8.35	0.4	25.7	5.11

The simulated  $S$ -parameters of the proposed FPD are shown in Fig. 4. It can be seen from Fig. 4(a) that the DB-FPD generates four resonant modes and four TZs in the required frequency band. According to the above analysis, the positions of  $f_{e1}$ ,  $f_{e2}$ ,  $f_{o1}$ , and  $f_{o2}$  can be adjusted by changing the corresponding parameters of the SLMR. In order to improve the isolation of the DB-FPD, two isolation resistors  $R_1$  and  $R_2$  are introduced into the circuit, and their influence on the isolation of the two passbands is analyzed. As shown in Fig. 4(b), it is found that  $R_1$  mainly affects the isolation of passband-1, while  $R_2$  mainly affects the isolation of passband-2. Finally, after simulation optimization, the resistance values of  $R_1$  and  $R_2$  are obtained as  $R_1 = 350 \Omega$  and  $R_2 = 100 \Omega$ , respectively, and the isolation between the two output ports are better than 25 and 14 dB respectively at passband-1 and passband-2.

#### 4. ANALYSIS OF TZS OF DB-FPD

In order to demonstrate the TZs generation mechanism of the DB-FPD, the effects of the relevant parameters on the TZs are analyzed. As shown in Fig. 4(a), TZ<sub>1</sub> and TZ<sub>2</sub> are controlled by the  $L_{f1}$  and  $L_{f2}$  loaded on the feeding structure. As shown in Fig. 5(a) and Fig. 5(b), when  $L_{f1}$  increases, the frequency of TZ<sub>1</sub> decreases, while the frequencies of the rest TZs remain unchanged. However, the frequency of TZ<sub>2</sub> varies with  $L_{f2}$ , and the frequencies of other TZs are not affected.

In addition, according to Fig. 1(b), the proposed SLMR can produce two TZs, that is TZ<sub>3</sub> and TZ<sub>4</sub> shown in Fig. 4(a). Through the simulation analysis, it is found that the location of two TZs can be adjusted by the length of  $L_{s1}$  and  $T_s$  on the SLMR, respectively. As shown in Fig. 6(a) and Fig. 6(b), it can be seen that as  $L_{s1}$  increases, the frequency of TZ<sub>3</sub> decreases, while the frequencies of other TZs are not affected. When  $T_s$  increases, the frequency of TZ<sub>4</sub> decreases, but no effect on the other TZs.

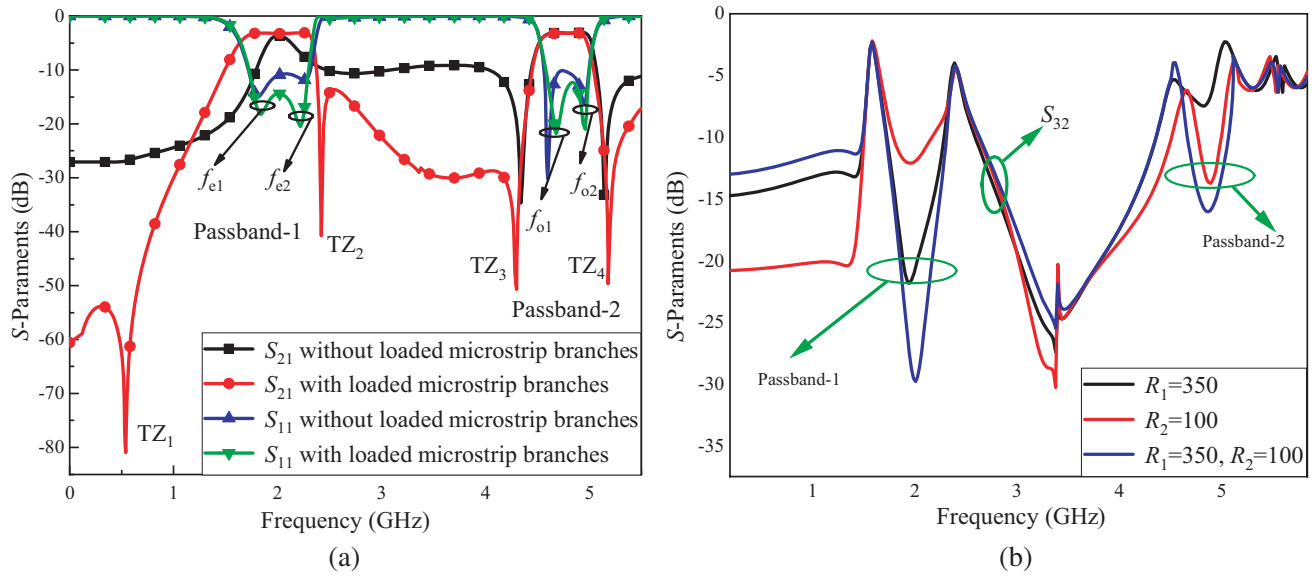


**Figure 4.**  $S$ -parameter simulation results of DB-FPD. (a)  $S_{11}$  and  $S_{21}$  with/without branches. (b)  $S_{32}$  with  $R_1$  or/and  $R_2$ .

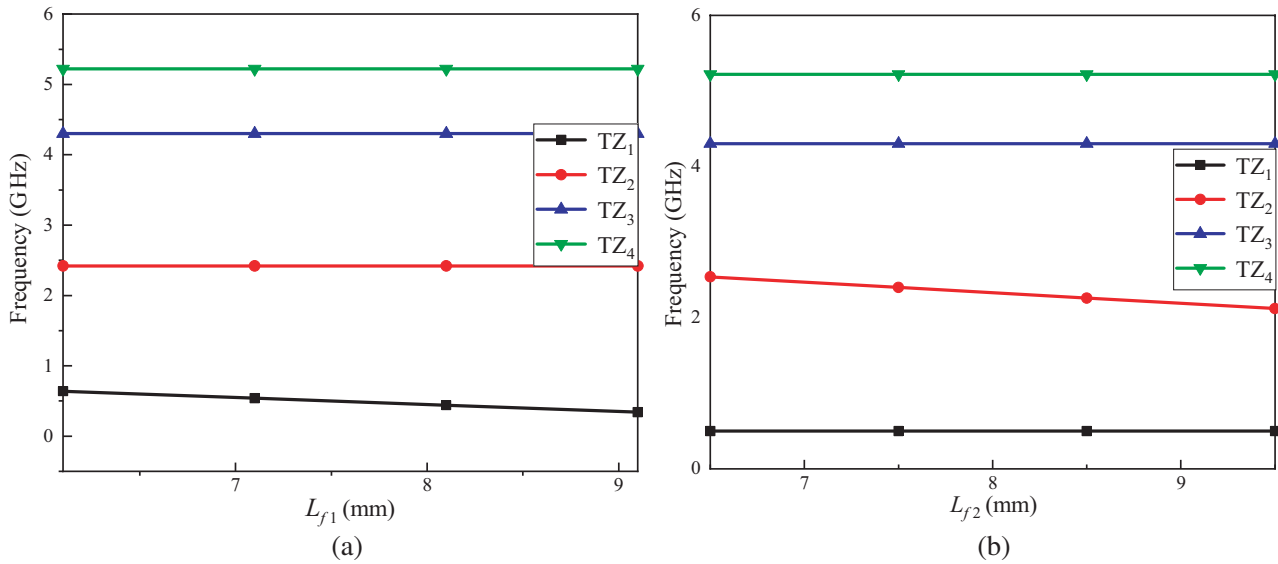


**Figure 5.** Variation of TZs with important parameters of DB-FPD. (a) Variation of TZs with  $L_{f1}$ . (b) Variation of TZs with  $L_{f2}$ .

### 5. RESULTS AND DISCUSSION

The proposed DB-FPD adopts an AD450L substrate with relative dielectric constant of 4.4 and thickness of 0.762 mm. In order to verify the validity of the design, a prototype of the proposed DB-FPD is fabricated and measured, Fig. 7 shows the measured and simulated  $S$ -parameters of the DB-FPD. It can be seen from Fig. 7(a) and Fig. 7(b) that the measured and simulated results are in good agreement. The measured center frequencies of the two passbands are 2.01 and 4.79 GHz, with the 3-dB fractional bandwidths of 29.7% and 7.99%, respectively. Correspondingly, the measured insertion losses at passband-1 and passband-2 are 3.10 and 3.17 dB, while the return losses are better than 15.86 and

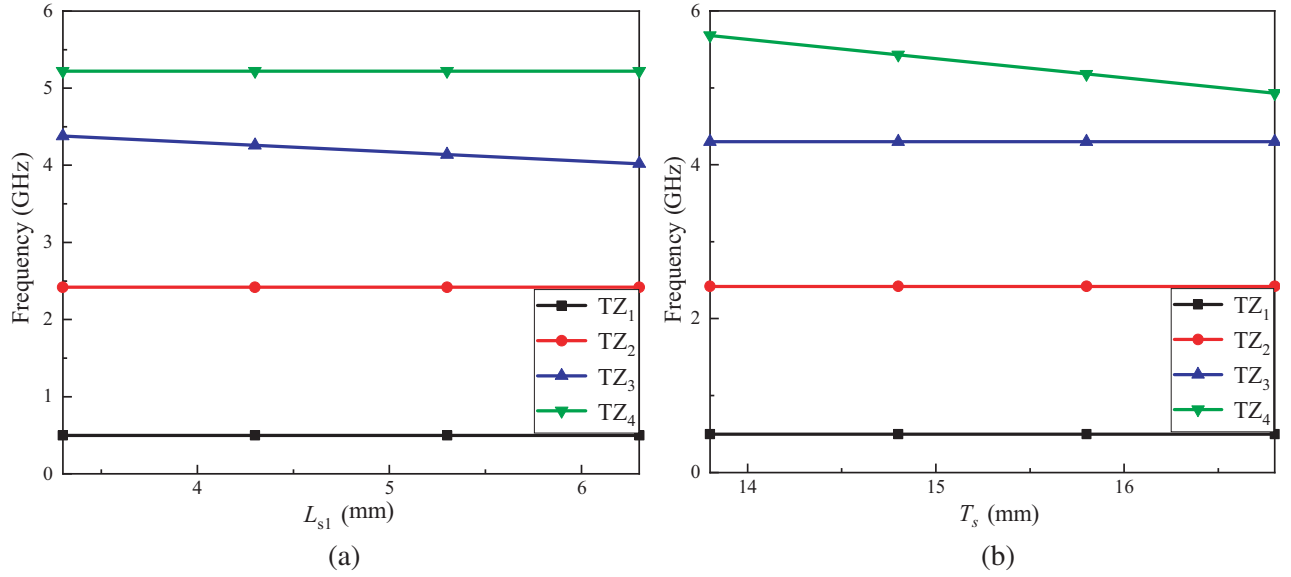


**Figure 6.** Variation of TZs with important parameters of DB-FPD. (a) Variation of TZs with  $L_{s1}$ . (b) Variation of TZs with  $T_s$ .

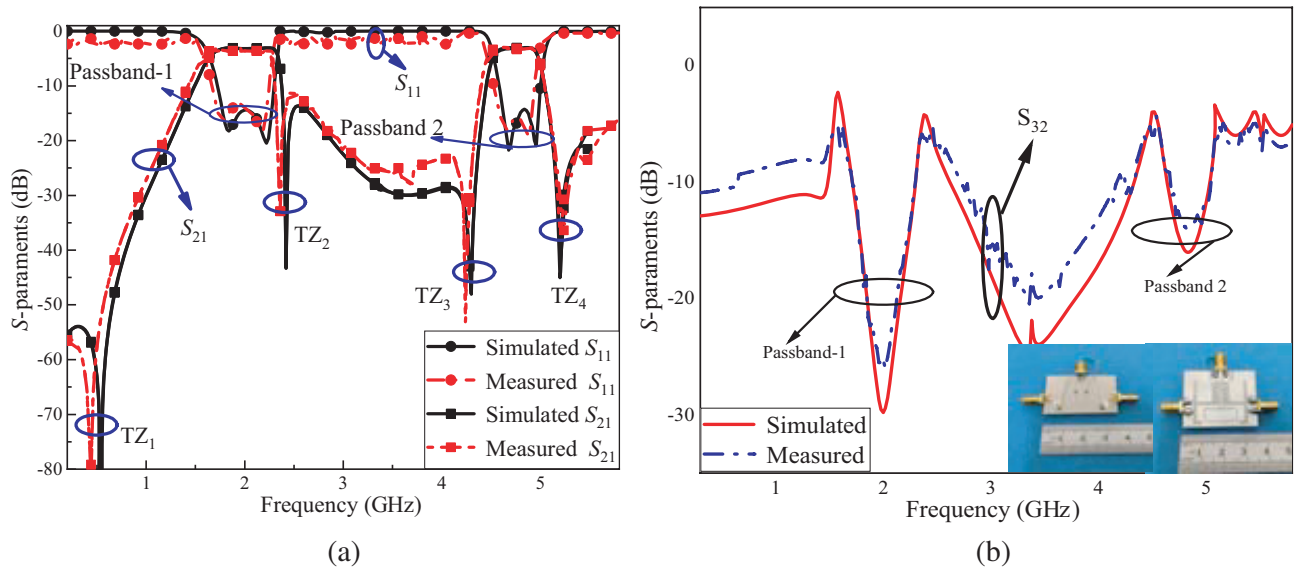


**Figure 7.** Measured and Simulated  $S$ -parameters of the Prototype. (a)  $S_{11}$  and  $S_{21}$ . (b)  $S_{32}$ .

**Table 2.** Compared with previous FPDs.

Ref.	$f_L/f_H$ (GHz)	FBW (%)	Number of TZs	In-band Isolation (dB)	In-band IL (dB)	In-band RL (dB)	Size ( $\lambda_g * \lambda_g$ )
[2]	5.5/8.3	14.5/9.6	2	> 20/20	3.9/4.5	14/22	2.15 * 0.89
[6]	1.8/2.96	8/7.4	3	> 8/10	3.8/3.9	10/15	0.28 * 0.57
[7]	3.5/5	7.4/4.2	1	> 8/6	3.9/4.9	13/15	0.35 * 0.27
This Work	2.01/4.79	29.7/7.99	4	> 28/14	3.10/3.17	15.86/15.12	0.49 * 0.42

15.12 dB, respectively. Meanwhile, the isolations in two passbands between the output ports are better than 25 and 14 dB, respectively.

Table 2 gives a comparison of the proposed DB-FPD with other reference works. It can be seen that this divider has the advantages of wider bandwidths, more TZs, lower insertion loss, and higher return loss.

## 6. CONCLUSION

In this letter, a DB-FPD is implemented using a multimode resonator. After the parameter optimization of SLMR, the FPD realizes two frequency bands with wider bandwidth. In addition, four individually controllable TZs are generated by using the resonance characteristics of the SLMR and the stubs loaded on the feeding network, which effectively improves the out-of-band suppression level of the two passbands. The center frequencies of the two passbands of the proposed DB-FPD are at 2.01 and 4.79 GHz, respectively. The measured fractional bandwidths are 29.7% and 7.99%, respectively, and the isolation in the two passbands is good, reaching 25 and 14 dB, respectively. The designed DB-FPD with lower insertion loss and wider bandwidth in each passband is very suitable for WiMax communication systems.

## ACKNOWLEDGMENT

This work was supported in part by the National Science Foundation of China under Grant 61661021 and 61901170, in part by the Natural Science Foundation of Jiangxi Province under Grant 20202BABL202008 and the Science and Technology Plan Project of Jiangxi Province under Grant 20202ACBL212002, 20204BCJ23007.

## REFERENCES

1. Chen, C. F., K. W. Zhou, R. Y. Chen, et al., "A compact quadruplexer-integrated filtering power divider," *IEEE Journal of Microwaves*, Vol. 1, No. 3, 804–809, 2021.
2. Wang, Y., C. Zhou, K. Zhou, et al., "Compact dual-band filtering power divider based on SIW triangular cavities," *Electronics Letters*, Vol. 54, No. 18, 1072–1074, 2018.
3. Chen, C. J., "A coupled-line isolation network for the design of filtering power dividers with improved isolation," *IEEE Transactions on Components, Packaging and Manufacturing Technology*, Vol. 8, No. 10, 1830–1837, 2018.
4. Deng, P. H. and L. C. Dai, "Unequal Wilkinson power dividers with favorable selectivity and high-isolation using coupled-line filter transformers," *IEEE Transactions on Microwave Theory and Techniques*, Vol. 60, No. 6, 1520–1529, 2012.
5. Zhang, G., Y. Liu, E. Wang, et al., "Multilayer packaging SIW three-way filtering power divider with adjustable power division," *IEEE Transactions on Circuits and Systems II: Express Briefs*, Vol. 67, No. 12, 3003–3007, 2020.
6. Li, Y. C., Q. Xue, and X. Y. Zhang, "Single- and dual-band power dividers integrated with bandpass filters," *IEEE Transactions on Microwave Theory and Techniques*, Vol. 61, No. 1, 69–76, 2012.
7. Li, Q., Y. Zhang, and Y. Fan, "Dual-band in-phase filtering power dividers integrated with stub-loaded resonators," *IET Microwaves, Antennas & Propagation*, No. 7, 695–699, 2015.
8. Zhang, G., X. Wang, and J. Yang, "Dual-band microstrip filtering power divider based on one single multimode resonator," *IEEE Microwave And Wireless Components Letters*, Vol. 28, No. 10, 891–893, 2018.
9. Li, Q., Y. Zhang, and C. T. M. Wu, "High-selectivity and miniaturized filtering Wilkinson power dividers integrated with multimode resonators," *IEEE Transactions on Components, Packaging and Manufacturing Technology*, Vol. 7, No. 12, 1990–1997, 2017.

10. Jia, X., S.-J. Fang, H. Liu, and Z. Wang, "Compact dual-band Wilkinson power divider terminated with frequency-dependent complex impedances," *Progress In Electromagnetics Research Letters*, Vol. 91, 85–91, 2020.
11. Wu, L., S. Wang, L. Li, and C. Tang, "Compact microstrip UWB power divider with dual notched bands using dual-mode resonator," *Progress In Electromagnetics Research Letters*, Vol. 75, 39–45, 2018.
12. Ren, B., H. Liu, Z. Ma, et al., "Compact dual-band bandpass filter and diplexer using hybrid resonant structure with independently controllable dual passbands," *International Journal of RF and Microwave Computer-Aided Engineering*, Vol. 29, No. 1, e21435, 2019.